Chinese Journal of Natural Medicines

New *nor*-*ent*-halimane and *nor*-clerodanediterpenes from *Callicarpa integerrima* with anti-MRSA activity

Mengru WANG, Qi WANG, Yanzi MA, Muhammad Aurang ZEB, Xiaoli LI, Feng SHEN, Weilie XIAO

Citation: Mengru WANG, Qi WANG, Yanzi MA, Muhammad Aurang ZEB, Xiaoli LI, Feng SHEN, Weilie XIAO, New *nor*-*ent*-halimane and *nor*-clerodanediterpenes from *Callicarpa integerrima* with anti-MRSA activity, Chinese Journal of Natural Medicines, 2024, 22(11), 1-8. doi: 10.1016/S1875-5364(24)60575-3.

View online: https://doi.org/10.1016/S1875-5364(24)60575-3

Available online at www.sciencedirect.com
ScienceDirect
Chinese Journal of Natural Medicines 2024, **22**(11): 1003-1010
doi: 10.1016/S1875-5364(24)60575-3
Chinese Journal of Natural Medicines

•Original article•

New *nor-ent*-halimane and *nor*-clerodane diterpenes from *Callicarpa integerrima* with anti-MRSA activity

WANG Mengru[1Δ], WANG Qi[2Δ], MA Yanzi[1, 4], ZEB Muhammad Aurang[1], LI Xiaoli[1*], SHEN Feng[3*], XIAO Weilie[1, 4*]

[1] *Key Laboratory of Medicinal Chemistry for Natural Resource, Ministry of Education, Yunnan Characteristic Plant Extraction Laboratory, Yunnan Key Laboratory of Research and Development for Natural Products, State Key Laboratory for Conservation and Utilization of Bio-Resources in Yunnan, School of Pharmacy and School of Chemical Science and Technology, Yunnan University, Kunming 650500, China;*

[2] *State Key Laboratory of Microbial Metabolism, School of Life Sciences and Biotechnology, Shanghai Jiao Tong University, Shanghai 200240, China;*

[3] *School of Biomedical Engineering, Shanghai Jiao Tong University, Shanghai 200030, China;*

[4] *Southwest United Graduate School, Kunming 650592, China*

Available online 20 Nov., 2024

[ABSTRACT] Two new *nor-ent*-halimane diterpenes and three previously unreported *nor*-clerodane diterpenes, designated callicaintides A−E (**1**−**5**), were isolated from *Callicarpa integerrima*. Compounds **1** and **2** feature a distinctive 5/6-membered ring system, while compounds **3**−**5** are characterized by progressively truncated carbon skeletons, containing 18, 17, and 16 carbons, respectively. In addition, four known compounds **6**−**9** were also identified. Their structures were elucidated using advanced spectroscopic techniques, including nuclear magnetic resonance (NMR), high-resolution electrospray ionization mass spectrometry (HR-ESI-MS), ultraviolet (UV), infrared radiation (IR), optical rotatory dispersion (ORD), DP4$^+$ analysis and electronic circular dichroism (ECD), supported by quantum chemical calculations. Compounds **1**−**9** were evaluated for their anti-MRSA activity. Among them, compound **6** demonstrated significant anti-MRSA activity, with a minimum inhibitory concentration (MIC) of 16 μg·mL^{-1}.

[KEY WORDS] *Callicarpa integerrima*; Halimane diterpenes; Clerodane diterpenes; Structure elucidation; anti-MRSA
[CLC Number] R917 **[Document code]** A **[Article ID]** 2095-6975(2024)11-1003-08

Introduction

Methicillin-resistant *Staphylococcus aureus* (MRSA) is a significant antibiotic-resistant pathogen responsible for a wide range of infections worldwide [1]. MRSA has developed resistance to almost all categories of antimicrobial agents [2], with only a few medications, such as vancomycin and teicoplanin, demonstrating efficacy against MRSA [3]. However, both low- and high-level resistance to these drugs is gradually increasing in clinical settings [4]. Consequently, there is a pressing need to discover novel antibacterial agents and innovative strategies to combat MRSA [5]. Medicinal plants have been utilized for treating various ailments since ancient times [6]. The relatively low toxicity of plant-derived natural products has established them as a crucial source for new drug development [6-8]. Numerous small molecules from medicinal plants have been identified as potent anti-MRSA lead compounds [7, 9]. For instance, naphthoquinone-derived heterodimers from *Eleutherine americana* bulbs [10] and diterpenes isolated from *Coleus blumei* Benth [11] have demonstrated significant antimicrobial activity.

Callicarpa integerrima, a vine or creeping shrub, is predominantly found at elevations ranging from 200 to 700 meters in Guangdong, Guangxi, Fujian, and Jiangxi provinces. Recent studies have documented the isolation of diterpenoids and phenylethanoid glycosides from this spec-

[Received on] 20-Feb.-2024
[Research funding] This work was supported by the National Natural Science Foundation of China (Nos. 22477108, 82260682), the Program for Changjiang Scholars and Innovative Research Team in University (No. IRT_17R94), the Project of Yunnan Characteristic Plant Screening and R&D Service CXO Platform (No. 2022YKZY001), and the Scientific Research Fund of Yunnan Provincial Department of Education (No. 2023Y0235).
[*]**Corresponding author]** E-mails: lixiaoli@ynu.edu.cn (LI Xiaoli); feng.shen@sjtu.edu.cn (SHEN Feng); xiaoweilie@ynu.edu.cn (XIAO Weilie)
[Δ]These authors contributed equally to this work.
These authors have no conflict of interest to declare.

ies [12-13]. Our previous investigation revealed the isolation of a series of novel diterpenoid compounds were isolated from *C. integerrima* [14].

To further investigate potential anti-MRSA substances from *C. integerrima*, we conducted a comprehensive study, focusing specifically on diterpenoid metabolites. In total, nine compounds were isolated and characterized, comprising five previously undescribed diterpenoids (**1**−**5**) and four known diterpenoids (**6**−**9**). Compounds **1**−**2** display a rare 5/6-membered ring system, representing a novel class of halimane diterpenes not previously reported. Compounds **3**−**5** are characterized as unusual *nor*-clerodane diterpenes, containing 18, 17, and 16 carbon atoms, respectively. This study details the biological activity of these compounds, with results indicating that compound 6 exhibits significant anti-MRSA efficacy.

Results and Discussion

Nine diterpenoids (**1**−**9**), comprising two novel *nor-ent*-halimane diterpenes and three *nor*-clerodane diterpenes (**1**−**5**), along with four previously identified compounds **6**−**9**, were isolated from the EtOAc-soluble fraction of *C. integerrima* (Fig. 1). Their structures were elucidated through comprehensive analysis of spectral data interpretation.

Compound **1** was isolated as a colorless oil with a molecular formula of $C_{19}H_{26}O_6$, as determined by high-resolution electrospray ionization mass spectrometry (HR-ESI-MS) (*m/z* 351.1802 $[M + H]^+$, Calcd. 351.1798) and nuclear magnetic resonance (NMR) data, indicating 7 degrees of hydrogen deficiency. The infrared radiation (IR) spectrum revealed absorption bands for hydroxy (3458 cm^{-1}) and carbonyl (1743 cm^{-1}) groups. The ^1H and ^{13}C NMR spectra of **1** displayed one ester carbonyl group at δ_C 171.2 (C-15), one trisubstituted double signals bond (δ_H 5.78, H-14; δ_C 171.7, C-13; δ_C 115.1, C-14), and a hemiacetal carbon (δ_C 98.1, C-16) (Table 1), which are characteristic signals of an *α,β*-unsaturated-*γ*-hydroxybutyrolactone moiety [15]. The signal at δ_C 224.2 (C-2) indicated a keto carbonyl group. The signals at δ_C 91.5 (C-10) and δ_C 80.8 (C-5) confirmed the presence of a 5,10-epoxide, accounting for the extra oxygen and degree of unsaturation. Additionally, the remaining signals corresponded to four methyl groups, four methylene, one oxygenated methine, one methine, and four quaternary carbons (Tables 1 and 2). The presence of two rings in the molecule was implied by the remaining two degrees of unsaturation. The heteronuclear multiple bond correlation (HMBC) cross-peaks from H-12 to C-14, C-13, and C-16 confirmed the *γ*-hydroxy butyrolactone connection to C-12, while the HMBCs of H_3-18 and H_3-19 to C-2, and H_3-18 to C-19 indicated the two methyl groups linked to C-4. Furthermore, the HMBC cross-peaks from H_3-20 to C-8, C-10, and C-11 revealed that the 5/6-fused double-ring scaffolds were connected to C-11 (Fig. 2). Thus, the planar structure of **1** was established, demonstrating that compound **1** is an *ent*-halimanediterpenoid with a novel 5/6-membered ring system.

The relative configuration of **1** was determined through nuclear overhauser effect spectroscopy (NOESY) correlations. The correlations between H_3-17 and H_3-20 indicated that Me-17 and Me-20 were positioned on the same side. However, determining the relative configuration of **1** solely based on the NOESY spectrum proved challenging. To further confirm the relative configuration of **1**, NMR chemical shifts were calculated at the PCM/mPW1PW91/6-31 + G(d, p) level. The DP4$^+$ analysis results indicated that (5*S*, 10*S*, 12*S*, 16*R*)-**1** was the most probable candidate with 100.0% probability (Fig. 4) . The absolute configuration of **1** was sub-

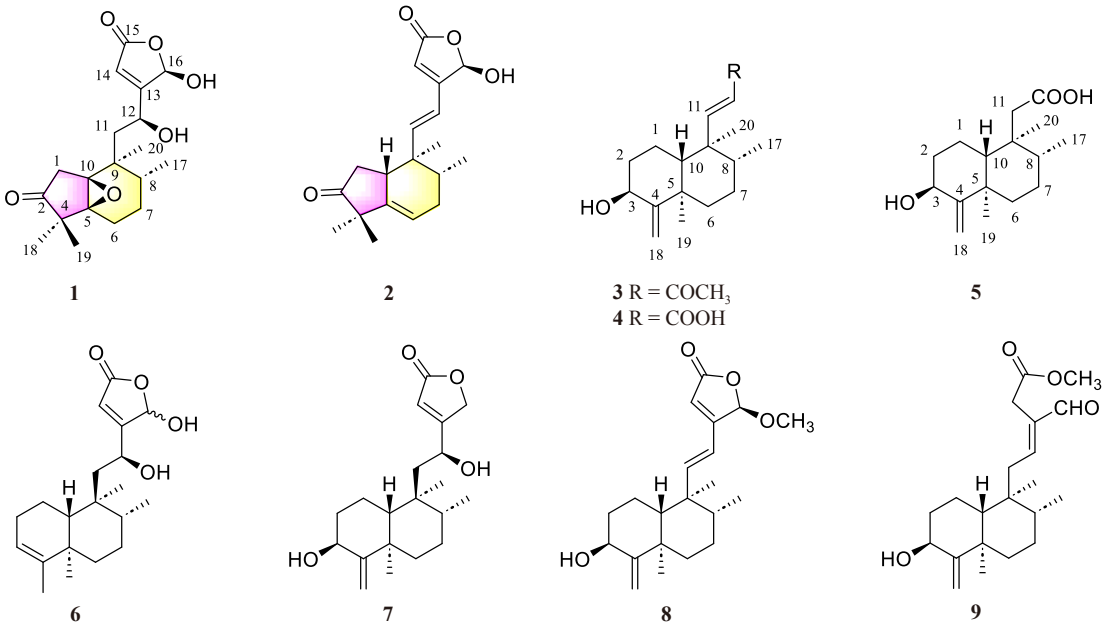

Fig. 1 Structures of compounds 1−9.

Table 1 ^{1}H NMR data (600 MHz) for compounds 1−5 in CD_3OD

No.	1	2	3	4	5
1a	2.90 d (16.7)	2.21 dd (18.7, 10.3)	1.62 dd (13.2, 3.7)	1.59 dd (12.9, 3.8)	1.85 d (12.5)
1b	2.03 d (16.7)	2.02 dd (18.7, 10.3)	1.38 m	1.41 m	1.52 m
2a			2.08 m	2.07 m	2.02 m
2b			1.18 overlap	1.15 m	1.13 m
3			4.24 dd (11.9, 5.4)	4.23 dd (12.0, 5.3)	4.15 dd (11.7, 5.2)
6a	2.01 m	5.49 q (3.3)	1.71 m	1.68 m	1.50 m
6b	1.54 m				
7a	1.87 m	2.15 m	1.58 m	1.57 m	1.39 m
7b	1.54 m	1.71 m			
8	1.80 m	1.79 m	1.46 m	1.39 m	1.75 m
10		2.91 m	1.18 overlap	1.10 m	1.29 m
11a	2.33 br s	6.33 d (16.4)	6.58 d (16.3)	6.53 d (15.8)	2.24 d (13.4)
11b	1.68 br s				2.16 d (13.4)
12a	4.94 t (8.7)	6.33 d (16.4)	6.00 d (16.3)	5.68 d (15.8)	
14	5.78 br s	5.87 s			
16	6.05 s	6.18 s			
17	1.00 d (6.6)	0.78 d (6.6)	0.75 d (6.6)	0.74 d (6.7)	0.82 d (6.5)
18a	1.20 s	1.01 s	4.97 s	4.95 s	4.82 s
18b			4.75 s	4.73 s	4.58 s
19	1.01 s	1.00 s	1.10 s	1.08 s	0.96 s
20	1.13 s	0.79 s	0.96 s	0.94 s	0.70 s
12-$COCH_3$			2.25 s		

sequently confirmed through electronic circular dichroism (ECD) analysis. The ECD spectrum of **1** corresponded well with the calculated curve, enabling the assignment of the absolute configuration of **1** as 5*S*, 8*R*, 9*S*, 10*S*, 12*S*, 16*R* (Fig. 6). Consequently, the structure of **1** was established and given the trivial name Callicaintide A.

Compound **2** was isolated as a colorless oil, and its molecular formula was determined to be $C_{19}H_{24}O_4$ with eight degrees of unsaturation by HR-ESI-MS (*m/z* 339.1573 $[M + Na]^+$, Calcd. for $C_{19}H_{24}O_4Na$ 339.1575). Detailed analysis and comparison of the ^{1}H and ^{13}C NMR data of **2** with those of compound **1** revealed that the main difference between them was the presence of the $\Delta^{11,12}$ double bond (δ_H 6.33, H-11; δ_H 6.33, H-12; δ_C 152.4, C-11; δ_C 118.6, C-12) instead of the hydroxyl group at C-12 (Tables 1 and 2), absence of the 5,10-epoxide found in compound **1**. The HMBCs (Fig. 2) from H-6 to C-5 and C-10 and from H_2-7 to C-5 indicated the presence of the $\Delta^{5,6}$ double bond. Based on this evidence, the planar structure of compound **2** was confirmed, as shown in Fig. 2. The NOESY correlations between H-10 and H-8 revealed that H-10 and H-8 were *β*-oriented (Fig. 3). However, the NOESY experiment did not provide all necessary correlations for a complete assignment of configuration. Therefore, the relative configuration of **2** was confirmed using theoretical NMR calculations and the DP4$^+$ probability (DP4$^+$ probability = 73.6%) (Fig. 5). Finally, the calculated ECD spectrum of **2** showed agreement with the experimental data, and the structure of **2** (8*R*, 9*R*, 10*R*, 16*R*) was determined by the biogenetic pathway and the calculated ECD, named Callicaintide B.

Compound **3** exhibited a quasi-molecular ion at *m/z* 299.1968 $[M + Na]^+$ (Calcd. for $C_{18}H_{28}O_2Na$, 299.1982) in the positive-ion HR-ESI-MS and was isolated as a colorless oil. The assignments of the ^{1}H and ^{13}C NMR data were determined through detailed analysis of its ^{1}H-^{1}H COSY, HSQC, and HMBC spectra, indicating that compound **3** could be a *nor*-diterpenoid. The ^{13}C NMR and DEPT spectra revealed eighteen signals, comprising four methyl groups, five methylene groups, five methines, and four non-protonated carbons (Table 1). The signal at C-3 (δ_C 70.2) suggested attachment to oxygen atoms. Additionally, two olefinic carbons at C-11 (δ_C 161.8) and C-12 (δ_C 130.7) were attributable to one double bond. Analysis of the 1D NMR data indicated that **3** possesses a skeleton similar to that of (3*S*, 5*R*, 8*R*,

Table 2 ^{13}C NMR data or compounds 1−5 in CD_3OD

No.	1	2	3	4	5
1	44.7	37.2	23.5	23.4	22.4
2	224.2	221.6	38.1	38.2	38.1
3			70.2	70.2	70.3
4	53.2	48.9	163.1	163.1	163.4
5	80.8	145.2	40.6	40.6	41.5
6	25.4	117.4	38.4	38.5	38.5
7	26.4	31.2	27.4	27.4	28.4
8	33.6	37.3	41.9	42.0	38.8
9	46.7	41.1	46.1	45.7	42.0
10	91.5	44.2	56.7	53.3	50.8
11	41.5	152.4	161.8	160.9	44.5
12	71.9	118.6	130.7	122.5	
13	171.7	162.8			
14	115.1	114.9			
15	171.2	172.4			
16	98.6	98.4			
17	15.6	15.4	17.0	17.0	16.7
18	21.7	21.1	100.6	100.6	100.2
19	19.0	25.4	21.5	21.5	21.6
20	15.2	7.4	12.4	12.4	17.6
11-COOH					176.5
12-$COCH_3$			201.4		
12-$COCH_3$			27.2		
12-COOH				172.0	

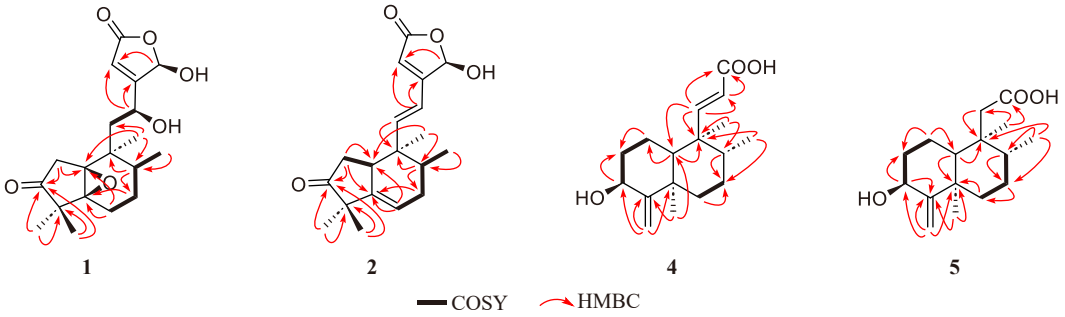

Fig. 2 Key HMBCs of compounds 1−2 and 4−5.

9*S*, 10*R*)-3,16-dihydroxycleroda-4(18),11(*E*),13(*Z*)-trien-15, 16-olide, a clerodane diterpenoid previously isolated from *Callicarpa arborea* [16]. The primary difference was the $COCH_3$ at C-12 in **3** replacing the typical *α*,*β*-unsaturated aldehyde group, confirmed by HMBCs from H-12 (δ_H 6.00) and H-11 (δ_H 6.58) to the ketone (δ_C 201.4) (Fig. 2). The relative configuration of **3** was determined based on NOESY correlations (Fig. 3), where correlations of H-3/H_3-19, H_3-17/H_3-20, and H_3-19/H_3-20 suggested that H-12, Me-17, Me-19, and Me-20 were *α*-oriented. NOESY cross-peaks of H-8/H-10 revealed their *β*-orientation. The final structure with absolute configuration (3*S*, 5*R*, 8*R*, 9*R*, 10*R*) was determined by ECD calculation (Fig. 6). Consequently, the structure of compound **3** was identified and trivially named Callicaintide C.

Compound **4** was isolated as a colorless powder with a molecular formula of $C_{17}H_{26}O_3$, as determined by the sodium adduct ions at *m/z* 277.1808 $[M - H]^+$ (Calcd. for $C_{17}H_{25}O_3$, 277.1809), indicating five indices of hydrogen deficiency. The ^{1}H and ^{13}C NMR spectra of **4** were similar to those of **3**, with the primary difference being the presence of a carboxyl group (δ_C 172.0) in **4** instead of the $COCH_3$ group

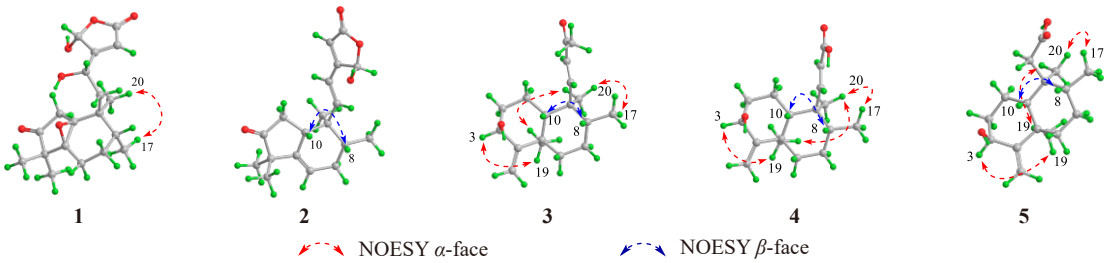

Fig. 3 Key ROESY correlations of compounds 1−5.

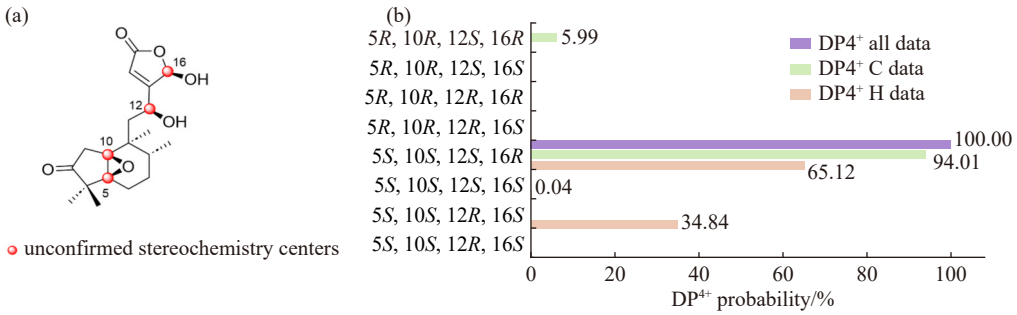

Fig. 4 (a) Unconfirmed stereochemistry centers of 1. (b) DP4$^+$ analysis of all possible diastereomers.

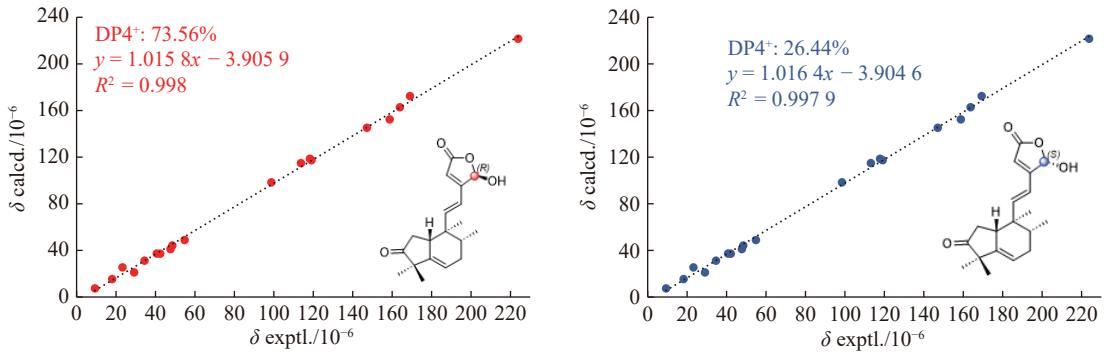

Fig. 5 Linear correlation between the experimental and calculated ^{13}C NMR chemical shifts and DP4$^+$ analysis of compound 2.

in **3** at C-12. As illustrated in Fig. 3, NOESY cross-peaks between H-8 and H-10 suggested that these protons were on the same side, arbitrarily assigned as *β* orientation. Conversely, NOESY cross-peaks between H-3/H_3-19, H_3-19/H_3-20, and H_3-17/H_3-20 indicated that H-3, Me-17, Me-19, and Me-20 were *α*-oriented. The absolute configuration of **4** was established as 3*S*, 5*R*, 8*R*, 9*R*, 10*R* through comparison of experimental and calculated ECD curves (Fig. 6). Consequently, the structure of compound **4** was elucidated and named Callicaintide D.

Compound **5** was isolated as a colorless powder. The molecular formula $C_{16}H_{27}O_6$ was established by the HR-ESI-MS at *m/z* 289.1775 $[M + Na]^+$ (Calcd. for $C_{16}H_{27}O_6Na$ 289.1774). Detailed 2D NMR analysis revealed that the structure of **5** resembled that of **4** in terms of the ring system but differed in the side chain. This inference was corroborated by HMBCs from the methylene to C-9 and C-20 and from the carboxyl to C-11, indicating the methylene linked to C-9 and the carboxyl linked to C-11. NOESY correlations of H-3/H_3-19/H_3-20/H_3-17 and H-8/H-10 were utilized to determine the *α*-orientation of CH_3-17, CH_3-19, and CH_3-20, and the *β*-orientation of the hydroxyl (C-3), H-8, and H-10. The absolute configuration (3*S*, 5*R*, 8*R*, 9*R*, 10*R*) of **5** was determined by the biogenetic pathway and ECD (Fig. 6). Consequently, the structure of **5** was confirmed and named Callicaintide E.

Additionally, four previously identified clerodane diterpenes were isolated and confirmed through a comparison of their spectral data with published literature. The known compounds (**6**−**9**) were characterized as 12(*S*),16ξ-dihydroxycleroda-3,13-dien-15,16-olide (**6**) [17], 3*β*,12(*S*)-Dihydroxycleroda-4(18),13-dien-15,16-olide (**7**) [17], (3*S*, 5*R*, 8*R*, 9*S*, 10*R*, 12*S*, 16*R*)-16-methoxy-3,12-dihydroxy-cleroda-4(18),13(*Z*)-dien-15,16-olide (**8**) [16], and (3*S*, 5*R*, 8*R*, 9*S*, 10*R*)-3-hydroxycleroda-4(18),12(*E*)-dien-15-methoxycarbonyl-16-al (**9**) [16].

All isolates (**1**−**9**) underwent evaluation for their anti-MRSA activity. Compound **6** exhibited notable efficacy, demonstrating a minimum inhibitory concentration (MIC) value of 16 μg·mL^{-1} (Fig. 7a). To further elucidate its mechanism of action, membrane permeability was analyzed using

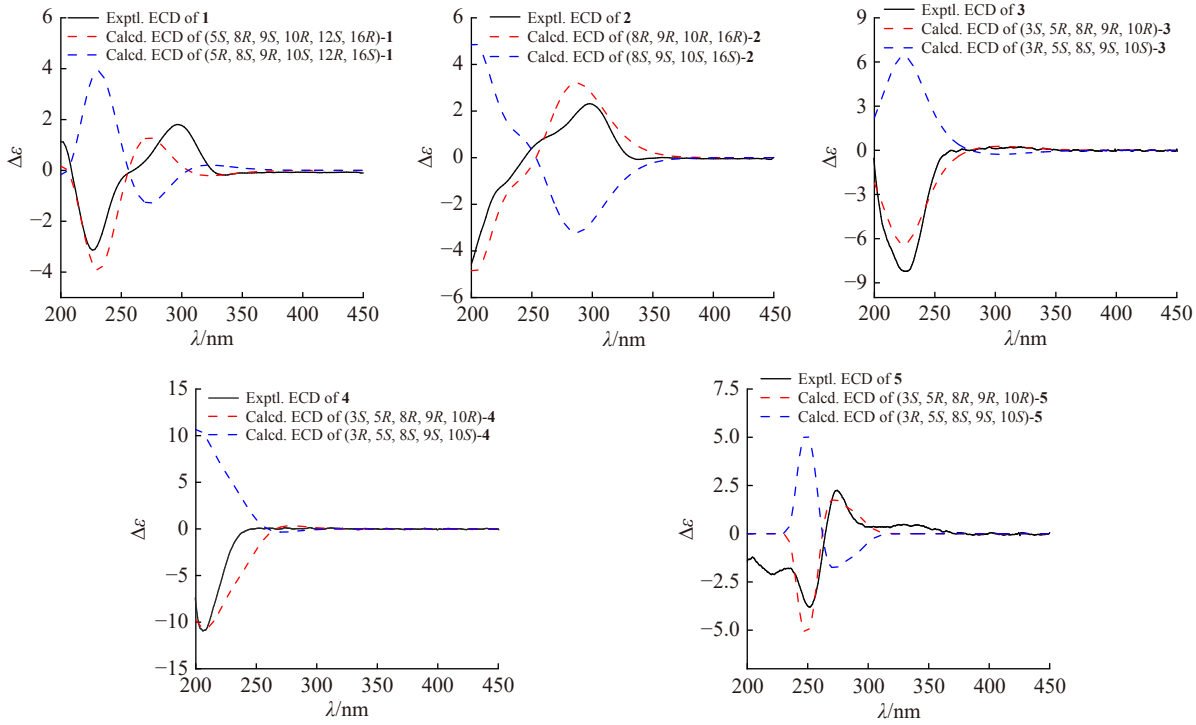

Fig. 6 Experimental and calculated ECD spectra of compounds 1−5.

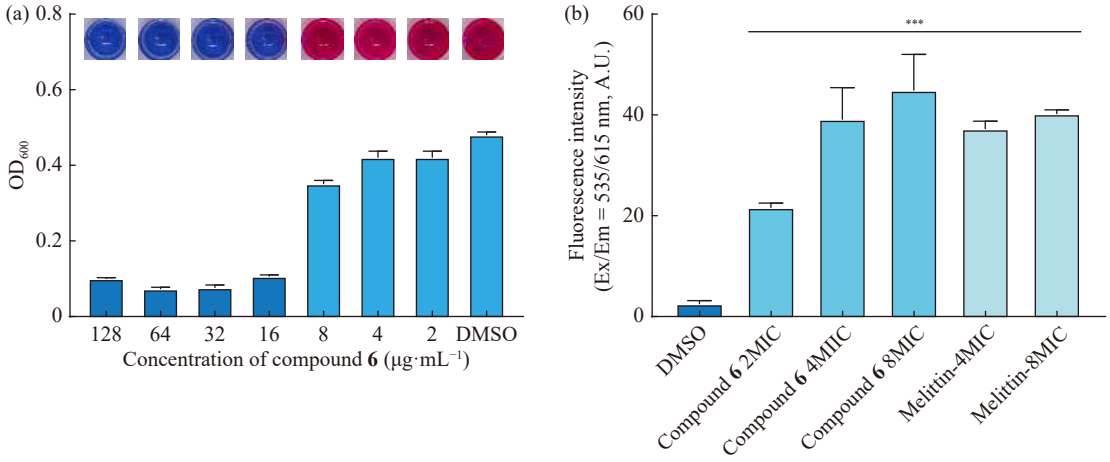

Fig. 7 (a) MIC values for compound 6, resazurin is reduced to pink when bacterial growth is not inhibited. (b) Increased membrane permeability of MRSA after treatment with (2 ×, 4 ×, and 8 × MIC) compound 6 and 4 × and 8 × MIC positive compound melittin.

propidium iodide (PI) [18]. The absorbance of MRSA treated with compound **6** increased markedly in a dose-dependent manner, corroborating that compound **6** compromised the membrane integrity of MRSA.

Experimental

General experimental procedures

Optical rotation values were determined using a Rudolph AP-IV polarimeter from Rudolph Research Analytical in Hackettstown, USA. Ultraviolet (UV) spectra were recorded using a Shimadzu UV-2401PC spectrophotometer. IR spectra were obtained from a VERTEX 70 FT-IR spectrometer. NMR spectra were measured on a Bruker Ascend^{TM} 600 MHz NMR instrument (Bruker, Karlsruhe, Germany). HR-ESI-MS data of the isolated compounds were acquired on a Thermo Scientific TSQ Endura mass spectrometer (Thermo, USA). Semi-preparative HPLC was performed on an Agilent 1260 Infinity II instrument (Agilent Technologies Inc., Waldbronn, Germany) coupled with a Zorbax SB-C_{18} column (5 μm, 9.4 mm × 250 mm) (Agilent Technologies Inc., California, USA). Column chromatography (CC) was conducted with silica gel (80−100 or 200−300 mesh, Qingdao Haiyang Chemical Co., Ltd.), MCI gel (CHP20/P120), reversed-phase C18 (RP-C_{18}) (S-50 μm, 12 nm, YMC Co., Ltd.), and Sepha-

dex LH-20 gel (Amersham Biosciences). Pre-coated silica gel GF_{254} plates were used for thin-layer chromatography (TLC) monitoring (Qingdao Haiyang Chemical Co., Ltd., Qingdao, China). Circular dichroism (ECD) spectra were obtained using the Gaussian 09 method.

Plant material

Twigs and leaves of *Callicarpa integerrima* were collected in March 2019 from Yuanyang, located in the Honghe Continental District of Yunnan Province, China.

The plant material was identified by CHEN Yu from the Kunming Institute of Botany, Chinese Academy of Sciences. A voucher specimen (YUN20190316) was deposited at the Key Laboratory of Medicinal Chemistry for Natural Resources, Ministry of Education, Yunnan University.

Extraction and isolation

A total of 20 kg of shade-dried twigs and leaves of *C. integerrima* underwent extraction with 95% methanol (3 × 30 L × 1 d) at room temperature, yielding a crude extract (4.0 kg) after evaporation under reduced pressure. The remaining methanol extract was dissolved in water and subjected to three successive partitions with ethyl acetate, resulting in respective extracts. The ethyl acetate-soluble extract (2.0 kg) underwent silica gel column chromatography (80−100 mesh; petroleum ether/ethyl acetate 10 : 1, 6 : 1, 4 : 1, 2 : 1, 1 : 1, *V/V*), yielding six fractions (Fr. A−Fr. F). Fraction E (178.3 g) was subjected to MCI gel column chromatography, using a gradient of MeOH/H_2O (from 0 : 100 to 100 : 0, *V/V*), leading to seven fractions (Fr. G1−Fr. G7). Fraction G4 (24.0 g) underwent ODS column chromatography, employing a gradient of MeOH/H_2O (from 50 : 50 to 100 : 0, *V/V*), resulting in six subfractions (Fr. G4.1−Fr.G4.6). Fraction G4.3 (8.3 g) was run on a Sephadex LH-20 column using MeOH to yield four fractions (Fr. G4.3.1−Fr. G4.3.4), which were subsequently purified through semi-preparative HPLC (48% ACN/H_2O), resulting in compounds **3** (1.8 mg), **4** (2.9 mg), and **5** (1.0 mg). Fraction G4.5 (5.9 g) underwent silica gel column chromatography and was eluted with $CHCl_2$/CH_3COCH_3 (5 : 1 *V/V*), yielding eight fractions (Fr. G4.5.1−Fr. G4.8). Fraction G4.5.2 (123.0 mg) was further separated through semi-preparative HPLC (3.0 mL·min^{-1}, CH_3OH/H_2O, 82 : 12 *V/V*), resulting in compounds **1** (3.7 mg), **2** (2.1 mg), **6** (8.3 mg), **7** (5.3 mg), **8** (4.5 mg), and **9** (36.3 mg).

Callicaintide A (**1**): Colorless oil; $[\alpha]_D^{25}$ +21.4 (*c* 0.05, MeOH λ_{max} (log ε) 226 (3.28); IR (ν_{max}): 3458, 2962, 2929, 1743 cm^{-1}; ^{1}H NMR data (Table 1) and ^{13}C NMR data (Table 2). HR-ESI-MS *m/z* 351.1802 $[M + H]^+$ (Calcd. for $C_{19}H_{27}O_6$, 351.1798).

Callicaintide B **(2)**: Colorless oil; $[\alpha]_D^{25}$ +44.4 (*c* 0.05, MeOH λ_{max} (log ε) 266 (3.71); IR (ν_{max}): 3350, 2964, 2927, 1741 cm^{-1}; ^{1}H NMR data (Table 1) and ^{13}C NMR data (Table 2). HR-ESI-MS *m/z* 339.1578 $[M + Na]^+$ (Calcd. for $C_{19}H_{27}O_6Na$, 339.1575).

Callicaintide C **(3)**: Colorless oil; $[\alpha]_D^{25}$ −18.2 (*c* 0.07, MeOH λ_{max} (log ε) 230 (3.78); IR (ν_{max}): 3452, 2929, 2865, 1737, 1672 cm^{-1}; ^{1}H NMR data (Table 1) and ^{13}C NMR data (Table 2). HR-ESI-MS *m/z* 299.1968 $[M + Na]^+$ (Calcd. for $C_{18}H_{28}O_2Na$, 299.1982).

Callicaintide D **(4)**: Colorless oil; $[\alpha]_D^{25}$ −6.00 (*c* 0.03, MeOH λ_{max} (log ε) 259 (3.28); IR (ν_{max}): 3341, 2927, 2862, 1692, 1646 cm^{-1}; ^{1}H NMR data (Table 1) and ^{13}C NMR data (Table 2). HR-ESI-MS *m/z* 277.1808 $[M - H]^+$ (Calcd. for $C_{17}H_{25}O_3$, 277.1809).

Callicaintide E **(5)**: Colorless oil; $[\alpha]_D^{25}$ −13.3 (*c* 0.03, MeOH λ_{max} (log ε) 256 (3.78); IR (ν_{max}): 3354, 2922, 2859, 1754, 1650 cm^{-1}; ^{1}H NMR data (Table 1) and ^{13}C NMR data (Table 2). HR-ESI-MS *m/z* 289.1775 $[M + Na]^+$ (Calcd. for $C_{16}H_{27}O_6Na$, 289.1774).

Quantum chemistry calculations

The conformational analysis for the test compounds and their corresponding diastereoisomers with the opposite configuration was performed using the molecular mechanics force field (MMFF) within the Spartan14 software package. Furthermore, additional geometry optimization was performed at the B3LYP/6-31G (d, p) level of theory in methanol as the solvent using the PCM model, implemented in Gaussian 09 [19]. Frequency calculations were also conducted to determine the nature of the identified stationary points. The magnetic shielding constants (σ) were calculated using Gauge-Independent Atomic Orbital (GIAO) calculations for NMR chemical shifts through Density Functional Theory (DFT) at the PCM/mPW1PW91/6-31G (d, p) level of theory in MeOH [20, 21]. The reference standard, TMS, had its NMR chemical shifts computed at the same level for comparison. To calculate linear correlation coefficients (R^2), the computed NMR chemical shifts were linearly regressed against the experimental values. DP4$^+$ calculations were conducted using the Excel spreadsheets available on the freely accessible website sarotti-NMR.weebly.com [22], following Boltzmann weighting of the computed chemical shifts of each conformer. ECD calculations of the optimized conformers were performed at the B3LYP/6-31G(d,p) level with the PCM model to compare with the experimental CD spectra.

Anti-MRSA activity assay

Determination of minimal inhibition concentration (MIC) was conducted for the compounds and their derivatives following a standardized protocol [23]. A series of dilutions (4, 8, 16, 32, 64, 128 μg·mL^{-1}) were prepared in 96-well microtiter plates. MRSA [24] was introduced to the antibiotic-containing plates and incubated for 16 h at 37 °C. OD600 values were measured using a Biotek Synergy HT2 multi-mode reader to determine the MICs. For an enhanced visual representation of MIC values, an additional set of controls was included by adding 30 μg·mL^{-1} resazurin (Shanghai Aladdin Bio-Chem Technology Co., Ltd. Shanghai, China). All experiments were performed in triplicate.

MRSA was centrifuged and resuspended in phosphate-buffered saline (PBS) to adjust the bacterial suspensions to an OD600 of approximately 0.2, followed by the addition of compound 6 (final concentrations of 2 ×, 4 ×, and 8 × MIC).

The bacterial suspensions were incubated for 30 min at 37 °C in dark conditions. Subsequently, the suspensions were treated with PI (Beijing Solarbio Science and Technology Co., Ltd. Beijing, China) at a final concentration of 1 μg·mL^{-1}. Following a 30-min incubation period, fluorescence measurements were obtained using a SpectraMax Gemini XPS Microplate Reader (Molecular) with an excitation wavelength (Ex)/emission wavelength (Em) of 535/615 nm.

Supplementary Materials

Supplementary information can be obtained by contacting the corresponding authors *via* email.

References

[1] Aires-de-Sousa M. Methicillin-resistant *Staphylococcus aureus* among animals: current overview [J]. *Clin Microbiol Infect*, 2017, **6**(23): 373-380.

[2] Kumar V, Shetty P, Arunodaya HS, *et al*. Potential fluorinated anti-MRSA thiazolidinone derivatives with antibacterial, antitubercular activity and molecular docking studies [J]. *Chem Biodivers*, 2022, **2**(19): e202100532.

[3] Livermore DM. Antibiotic resistance in staphylococci [J]. *Int J Antimicrob Agents*, 2000, **16**: 3-10.

[4] Kavi J, Andrews JM, Wise R, *et al*. Mupirocin-resistant *staphylococcus aureus* [J]. *The Lancet*, 1987, **8573**(330): 1472-1473.

[5] Aslam B, Wang W, Arshad MI, *et al*. Antibiotic resistance: a rundown of a global crisis [J]. *Infect Drug Resist*, 2018, **11**: 1645-1658.

[6] Pandey AK, Kumar S. Perspective on plant products as antimicrobials agents: a review [J]. *Pharmacologia*, 2013, **7**(4): 469-480.

[7] Newman DJ, Cragg GM. Natural products as sources of new drugs from 1981 to 2014 [J]. *J Nat Prod*, 2016, **3**(79): 629-661.

[8] Zeng Q, Wang ZJ, Chen S, *et al*. Phytochemical and anti-MRSA constituents of *Zanthoxylum nitidum* [J]. *Biomed Pharmacother*, 2022, **148**: 112758.

[9] Che CT, Zhang HJ. Plant natural products for human health [J]. *Int J Mol Sci*, 2019, **4**(20): 830-834.

[10] Chen DL, Sun ZC, Liu YY, *et al*. Eleucanainones A and B: two dimeric structures from the bulbs of *Eleutherine americana* with anti-MRSA activity [J]. *Org Lett*, 2020, **9**(22): 3449-3453.

[11] Jurkaninová S, Kubínová R, Nejezchlebová M, *et al*. Anti-MRSA activity of abietane diterpenes from *Coleus blumei* Benth [J]. *Nat Prod Res*, 2019, **18**(35): 3033-3039.

[12] Pu DB, Zhang XJ, Bi DW, *et al*. Callicarpins, two Classes of rearranged *ent*-clerodane diterpenoids from *Callicarpa* plants blocking NLRP3 inflammasome-induced pyroptosis [J]. *J Nat Prod*, 2020, **7**(83): 2191-2199.

[13] Jiang W, Ma W, Guan J, *et al*. Integerrima A–E, phenylethanoid glycosides from the stem of *Callicarpa integerrima* [J]. *J Nat Med*, 2023, **3**(77): 496-507.

[14] Bi DW, Zhao YX, Qiu X, *et al*. Callicarpanes A–L, twelve new clerodane diterpenoids with NLRP3 inflammasome inhibitory activity from *Callicarpa integerrima* [J]. *Chem Biodivers*, 2023, **1**(20): e202200985.

[15] Xu J, Wang M, Liu Z, *et al*. Terpenoids from the *Sponge Sarcotragus* sp. collected in the south China sea [J]. *J Nat Prod*, 2023, **2**(86): 330-339.

[16] Pu DB, Lin J, Pu XJ, *et al*. The discovery of potentially active diterpenoids to inhibit the pyroptosis from *Callicarpa arborea* [J]. *Bioorg Chem*, 2022, **128**(2022): 106022.

[17] Jones WP, Lobo-Echeverri T, Mi Q, *et al*. Cytotoxic constituents from the Fruiting Branches of *Callicarpa americana* collected in southern florida [J]. *J Nat Prod*, 2007, **3**(70): 372-377.

[18] Pietschmann S, Hoffmann K, Voget M, *et al*. Synergistic effects of miconazole and polymyxin B on microbial pathogens [J]. *Vet Res Commun*, 2008, **6**(33): 489-505.

[19] Gaussian 09, Revision E. 01, M. J. Frisch, G. W. Trucks, H. B. Schlegel, G. E. Scuseria, M. A. Robb, J. R. Cheeseman, G. Scalmani, V. Barone, G. A. Petersson, H. Nakatsuji, X. Li, M. Caricato, A. Marenich, J. Bloino, B. G. Janesko, R. Gomperts, B. Mennucci, H. P. Hratchian, J. V. Ortiz, A. F. Izmaylov, J. L. Sonnenberg, D. Williams-Young, F. Ding, F. Lipparini, F. Egidi, J. Goings, B. Peng, A. Petrone, T. Henderson, D. Ranasinghe, V. G. Zakrzewski, J. Gao, N. Rega, G. Zheng, W. Liang, M. Hada, M. Ehara, K. Toyota, R. Fukuda, J. Hasegawa, M. Ishida, T. Nakajima, Y. Honda, O. Kitao, H. Nakai, T. Vreven, K. Throssell, J. A. Montgomery, Jr., J. E. Peralta, F. Ogliaro, M. Bearpark, J. J. Heyd, E. Brothers, K. N. Kudin, V. N. Staroverov, T. Keith, R. Kobayashi, J. Normand, K. Raghavachari, A. Rendell, J. C. Burant, S. S. Iyengar, J. Tomasi, M. Cossi, J. M. Millam, M. Klene, C. Adamo, R. Cammi, J. W. Ochterski, R. L. Martin, K. Morokuma, O. Farkas, J. B. Foresman, and D. J. Fox, Gaussian, Inc., Wallingford CT, 2016.

[20] Grimblat N, Sarotti AM. Computational chemistry to the rescue: modern toolboxes for the assignment of complex molecules by GIAO NMR calculations [J]. *Chem Eur J*, 2016, **35**(22): 12246-12261.

[21] Shi QQ, Zhang XJ, Wang TT, *et al*. Euphopias A–C: three rearranged jatrophane diterpenoids with tricyclo[8.3. $0.0^{(2,\ 7)}$]tridecane and tetracyclo[11.3. $0.0^{(2,\ 10)}$. $0^{(3,\ 7)}$]hexadecane cores from *Euphorbia helioscopia* [J]. *Org Lett*, 2020, **20**(22): 7820-7824.

[22] Grimblat N, Zanardi MM, Sarotti AM. Beyond DP4: an improved probability for the stereochemical assignment of isomeric compounds using quantum chemical calculations of NMR shifts [J]. *J Org Chem*, 2015, **24**(80): 12526-12534.

[23] Andrews JM. Determination of minimum inhibitory concentrations [J]. *J Antimicrob Chemother*, 2001, **suppl_1**(48): 5-16.

[24] Xu M, Zhang F, Cheng Z, *et al*. Functional genome mining reveals a class V lanthipeptide containing a d-amino acid introduced by an $F4_{20}H_2$ - dependent reductase [J]. *Angew Chem*, 2020, **41**(132): 18185-18191.

Cite this article as: WANG Mengru, WANG Qi, MA Yanzi, *et al*. New *nor*-*ent*-halimane and *nor*-clerodane diterpenes from *Callicarpa integerrima* with anti-MRSA activity [J]. *Chin J Nat Med*, 2024, **22**(11): 1003-1010.